Spectro−Temporal Characterization of the Photoactivation Mechanism of Two New Oxidized Cryptochrome/Photolyase Photoreceptors

Johanna Brazard,[†] Anwar Usman,[†] Fabien Lacombat,[†] Christian Ley,[†]
Monique M. Martin,[†] Pascal Plaza,*[,†] Laetitia Mony,[‡] Marc Heijde,[§]
Gérald Zabulon,[§] and Chris Bowler[§]

UMR 8640 CNRS-ENS-UPMC, Département de Chimie, Ecole Normale Supérieure, 24 rue Lhomond, 75005 Paris, France, UMR 8601 CNRS, Laboratoire de Chimie et Biochimie Pharmacologies et Toxicologiques, Université Paris Descartes, 12 rue de l'Ecole de médecine, 75006 Paris, France, and UMR 8186 CNRS-ENS, Département de Biologie, Ecole Normale Supérieure, 46 rue d'Ulm, 75005 Paris, France

Received January 20, 2010; E-mail: Pascal.Plaza@ens.fr

Abstract: The photoactivation dynamics of two new flavoproteins (OtCPF1 and OtCPF2) of the cryptochrome photolyase family (CPF), belonging to the green alga *Ostreococcus tauri*, was studied by broadband UV−vis femtosecond absorption spectroscopy. Upon excitation of the protein chromophoric cofactor, flavin adenine dinucleotide in its oxidized form (FAD_{ox}), we observed in both cases the ultrafast photoreduction of FAD_{ox}: in 390 fs for OtCPF1 and 590 fs for OtCPF2. Although such ultrafast electron transfer has already been reported for other flavoproteins and CPF members, the present result is the first demonstration with full spectral characterization of the mechanism. Analysis of the photoproduct spectra allowed identifying tryptophan as the primary electron donor. This residue is found to be oxidized to its protonated radical cation form ($WH^{\bullet+}$), while FAD_{ox} is reduced to $FAD^{\bullet-}$. Subsequent kinetics were observed in the picosecond and subnanosecond regime, mostly described by a biexponential partial decay of the photoproduct transient signal (9 and 81 ps for OtCPF1, and 13 and 340 ps for OtCPF2), with reduced spectral changes, while a long-lived photoproduct remains in the nanosecond time scale. We interpret these observations within the model proposed by the groups of Brettel and Vos, which describes the photoreduction of $FADH^{\bullet}$ within *E. coli* CPD photolyase (EcCPD) as a sequential electron transfer along a chain of three tryptophan residues, although in that case the rate limiting step was the primary photoreduction in 30 ps. In the present study, excitation of FAD_{ox} permitted to reveal the following steps and spectroscopically assign them to the hole-hopping process along the tryptophan chain, accompanied by partial charge recombination at each step. In addition, structural analysis performed by homology modeling allowed us to propose a tentative structure of the relative orientations of FAD and the conserved tryptophan triad. The results of preliminary transient anisotropy measurements performed on OtCPF2 finally showed good compatibility with the oxidation of the distal tryptophan residue (WH_{351}) in 340 ps, hence, with the overall Brettel−Vos mechanism.

1. Introduction

The cryptochrome/photolyase family (CPF) forms a group of structurally homologous proteins, widely distributed within eubacteria, archaea and eukaryotes. These proteins are activated by near-UV/blue photons and mediate a variety of light-dependent biological functions.[1−3] Photolyases use the energy of light to repair the major UV-induced lesions of DNA: CPD photolyases (CPD-PL) split cyclobutane pyrimidine dimers (CPD), while (6-4) photolyases (64-PL) take care of (6-4) pyrimidine−pyrimidone photoproducts.[4−7] Cryptochromes (CRY) may act as photosensory proteins mediating different types of responses to light:[8] regulation of photomorphogenesis, flowering and phototropism in plants,[9] synchronization of the circadian clock for some animals.[10] DASH cryptochromes (CRY-DASH) form a separate subfamily, the members of which have been proposed to perform distinct functions in different organisms:

† UMR 8640 CNRS-ENS-UPMC, Département de Chimie, Ecole Normale Supérieure.
‡ UMR 8601 CNRS, Laboratoire de Chimie et Biochimie Pharmacologies et Toxicologiques, Université Paris Descartes.
§ UMR 8186 CNRS-ENS, Département de Biologie, Ecole Normale Supérieure.

(1) Sancar, A. *Chem. Rev.* **2003**, *103*, 2203−2237.
(2) Cashmore, A. R.; Jarillo, J. A.; Wu, Y.-J.; Liu, D. *Science* **1999**, *284*, 760−765.
(3) Todo, T.; Ryo, H.; Yamamoto, K.; Toh, H.; Inui, T.; Ayaki, H.; Nomura, T.; Ikenaga, M. *Science* **1996**, *272*, 109−112.

(4) Malhotra, K.; Kim, S. T.; Sancar, A. *Biochemistry* **1994**, *33*, 8712−8718.
(5) Todo, T.; Takemori, H.; Ryo, H.; Ihara, M.; Matsunaga, T.; Nikaido, O.; Sato, K.; Nomura, T. *Nature* **1993**, *361*, 371−374.
(6) Brudler, R.; Hitomi, K.; Daiyasu, H.; Toh, H.; Kucho, K.; Ishiura, M.; Kanehisa, M.; Roberts, V. A.; Todo, T.; Tainer, J. A.; Getzoff, E. D. *Mol. Cell* **2003**, *11*, 59−67.
(7) Daiyasu, H.; Ishikawa, T.; Kuma, K.; Iwai, S.; Todo, T.; Toh, H. *Genes Cells* **2004**, *9*, 479−495.
(8) Lin, C. T.; Todo, T. *Genome Biology* **2005**, *6*, article number 220.
(9) Ahmad, M.; Cashmore, A. R. *Nature* **1993**, *366*, 162−166.
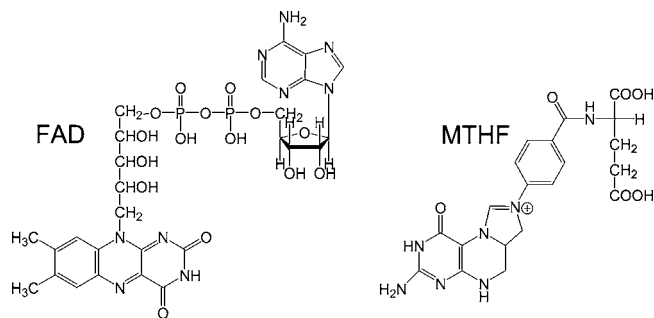(10) Sancar, A. *J. Biol. Chem.* **2004**, *279*, 34079−34082.

Figure 1. Chemical structures of flavin adenine dinucleotide (FAD, left) and 5,10-methenyl-tetrahydrofolate (MTHF, right).

transcriptional repression within the circadian system,[6,7,11] double-stranded DNA photolyase activity,[7] specific single-stranded DNA photolyase activity.[12−14]

All CPF proteins characterized to date noncovalently bind an essential cofactor, flavin adenine dinucleotide (FAD, Figure 1), which presents three oxidation states.[15] The biological functions of CPF proteins rely on the excitation of FAD either by direct photon absorption or through resonance energy transfer from a second noncovalently bound cofactor, a light-harvesting chromophore. This photoantenna is often 5,10-methenyl-tetrahydrofolate (MTHF, Figure 1) and sometimes 8-hydroxy-7,8-didemethyl-5-deazariboflavin (8-HDF) (see ref 1 for a review).

The photocatalytically active redox form of FAD in photolyases is $FADH^-$ (fully reduced form).[1] *In vitro* analyses showed that $FADH^-$ may be produced by photoreduction of $FADH^{\bullet}$ (semireduced form). This reaction, also called photoactivation, involves the intramolecular transfer of an electron from a redox active residue (tryptophan or tyrosine) to the excited flavin.[1,16−23] In the case of *Escherichia coli* CPD-PL (abbreviated EcCPD), the groups of Brettel and Vos showed that this reaction actually proceeds by ultrafast electron hopping along a chain of three tryptophan residues.[18−20,22−24] The excited $FADH^{\bullet}$ is first reduced by a nearby tryptophan (WH_{382}) in ∼30 ps, which is in turn reduced by an intermediate tryptophan (WH_{359}) in less than 9 ps. The oxidized WH_{359} is finally reduced in less than 30 ps by WH_{306}, which is exposed to the surface of the protein.

The tryptophan triad of EcCPD is actually very well conserved among CPF proteins,[1,25] and the electron-hopping mechanism was subsequently invoked by Kao et al. to interpret the photoinduced dynamics of several CPF proteins (three insect CRY, *Arabidopsis thaliana* 64-PL and EcCPD) bearing FAD_{ox}.[25] Exciting FAD_{ox} is particularly interesting because it was long known that photoreduction of FAD_{ox} by tryptophan or tyrosine in non-CPF flavoproteins can take place in the subpicosecond regime.[26−31] This is indeed what Kao et al. observed by femtosecond transient absorption spectroscopy, with primary photoreduction (reduction of the excited flavin by the proximal tryptophan, generically noted WH_p) lifetimes ranging from 0.5 to 1.8 ps.[25] Contrary to the case of EcCPD bearing $FADH^{\bullet}$, the rate limiting step was not the primary photoreduction anymore and subsequent kinetic steps could be resolved. The authors interpreted their results by the oxidized WH_p being reduced by the medium tryptophan (noted WH_m) with lifetimes ranging from 20 to 54 ps, while the oxidized WH_m is reduced by the distal tryptophan (noted WH_d) in the nanosecond regime.[25]

In the genome of the smallest known autotrophic eukaryote: the green alga *Ostreococcus tauri*,[32] the group of Bowler identified five CPF genes: three CPD-PL, one 64-PL and one CRY-DASH.[33] Since few studies were carried out on the photoactivation of 64-PL[25,34] and none was reported on CRY-DASH, we focused the present study on the photoactivation of two proteins of these subfamilies. OtCPF1 genetically groups with 64-PL and animal CRY, and OtCPF2 is a CRY-DASH. Both proteins bind FAD and OtCPF2 also contains MTHF.[33,35] Interestingly, OtCPF1 shows dual function: 64-PL activity and repression of circadian-clock-controlled gene expression.[33] OtCPF2 shows CPD-PL activity on double stranded DNA.[33]

We here report a thorough study of the primary events following excitation of FAD_{ox} in both OtCPF1 and OtCPF2, probed in real time by femtosecond broadband absorption spectroscopy. Our measurements provide full spectra of the reaction intermediates, thereby allowing their chemical identification. For this scope, we first made a quantitative determination of the FAD and MTHF content of OtCPF2 by steady-state absorption and fluorescence spectroscopy—the corresponding study of OtCPF1 has already been published.[35] In addition, homology modeling allowed us to propose a tentative structure of the relative orientations of FAD and the conserved

(11) Hitomi, K.; Okamoto, K.; Daiyasu, H.; Miyashita, H.; Iwai, S.; Toh, H.; Ishiura, M.; Todo, T. *Nucleic Acids Res.* **2000**, *28*, 2353–2362.

(12) Huang, Y. H.; Baxter, R.; Smith, B. S.; Partch, C. L.; Colbert, C. L.; Deisenhofer, J. *Proc. Natl. Acad. Sci. U.S.A.* **2006**, *103*, 17701–17706.

(13) Selby, C. P.; Sancar, A. *Proc. Natl. Acad. Sci. U.S.A.* **2006**, *103*, 17696–17700.

(14) Pokorny, R.; Klar, T.; Hennecke, U.; Carell, T.; Batschauer, A.; Essen, L. O. *Proc. Natl. Acad. Sci. U.S.A.* **2008**, *105*, 21023–21027.

(15) Massey, V. *Biochem. Soc. Trans.* **2000**, *28*, 283–296.

(16) Aubert, C.; Mathis, P.; Eker, A. P. M.; Brettel, K. *Biochemistry* **1999**, *96*, 5423–5427.

(17) Aubert, C.; Vos, M. H.; Mathis, P.; Eker, A. P. M.; Brettel, K. *Nature* **2000**, *405*, 586–590.

(18) Byrdin, M.; Eker, A. P. M.; Vos, M. H.; Brettel, K. *Proc. Natl. Acad. Sci. U.S.A.* **2003**, *100*, 8676–8681.

(19) Byrdin, M.; Sartor, V.; Eker, A. P. M.; Vos, M. H.; Aubert, C.; Brettel, K.; Mathis, P. *Biochim. Biophys. Acta Bioenerg.* **2004**, *1655*, 64–70.

(20) Byrdin, M.; Villette, S.; Eker, A. P. M.; Brettel, K. *Biochemistry* **2007**, *46*, 10072–10077.

(21) Byrdin, M.; Villette, S.; Espagne, A.; Eker, A. P. M.; Brettel, K. *J. Phys. Chem. B* **2008**, *112*, 6866–6871.

(22) Lukacs, A.; Eker, A. P. M.; Byrdin, M.; Brettel, K.; Vos, M. H. *J. Am. Chem. Soc.* **2008**, *130*, 14394–14395.

(23) Lukacs, A.; Eker, A. P. M.; Byrdin, M.; Villette, S.; Pan, J.; Brettel, K.; Vos, M. H. *J. Phys. Chem. B* **2006**, *110*, 15654–15658.

(24) Byrdin, M.; Lukacs, A.; Thiagarajan, V.; Eker, A. P. M.; Brettel, K.; Vos, M. H. *J. Phys. Chem. A* **2010**, *114*, 3207−3214.

(25) Kao, Y. T.; Tan, C.; Song, S. H.; Ozturk, N.; Li, J.; Wang, L. J.; Sancar, A.; Zhong, D. P. *J. Am. Chem. Soc.* **2008**, *130*, 7695–7701.

(26) Chosrowjan, H.; Taniguchi, S.; Mataga, N.; Tanaka, F.; Todoroki, D.; Kitamura, M. *J. Phys. Chem. B* **2007**, *111*, 8695–8697.

(27) Chosrowjan, H.; Taniguchi, S.; Mataga, N.; Tanaka, F.; Todoroki, D.; Kitamura, M. *Chem. Phys. Lett.* **2008**, *462*, 121–124.

(28) Mataga, N.; Chosrowjan, H.; Taniguchi, S.; Tanaka, F.; Kido, N.; Kitamura, M. *J. Phys. Chem. B* **2002**, *106*, 8917–8920.

(29) Nunthaboot, N.; Tanaka, F.; Kokpol, S.; Chosrowjan, H.; Taniguchi, S.; Mataga, N. *J. Photochem. Photobiol. A* **2009**, *201*, 191–196.

(30) Tanaka, F.; Chosrowjan, H.; Taniguchi, S.; Mataga, N.; Sato, K.; Nishina, Y.; Shiga, K. *J. Phys. Chem. B* **2007**, *111*, 5694–5699.

(31) Zhong, D. P.; Zewail, A. H. *Proc. Natl. Acad. Sci. U.S.A.* **2001**, *98*, 11867–11872.

(32) Courties, C.; Vaquer, A.; Trousselier, M.; Lautier, J.; Chretiennotdinet, M. J.; Neveux, J.; Machado, C.; Claustre, H. *Nature* **1994**, *370*, 255–255.

(33) Heijde, M.; Zabulon, G.; Corellou, F.; Ishikawa, T.; Brazard, J.; Usman, A.; Plaza, P.; Martin, M. M.; Falciatore, A.; Todo, T.; Bouget, F.-Y.; Bowler, C. *Plant Cell Environ.* Submitted.

(34) Weber, S.; Kay, C. W. M.; Mogling, H.; Mobius, K.; Hitomi, K.; Todo, T. *Proc. Natl. Acad. Sci. U.S.A.* **2002**, *99*, 1319–1322.

(35) Usman, A.; Brazard, J.; Martin, M. M.; Plaza, P.; Heijde, M.; Zabulon, G.; Bowler, C. *J. Photochem. Photobiol. B* **2009**, *96*, 38–48.

tryptophan triad. We finally report a study by femtosecond polarized absorption spectroscopy, a method applied by the groups of Brettel and Vos to the photoreduction of FADH[•] in EcCPD in order to resolve electron transfer between the tryptophan residues of the tryptophan chain, which are chemically identical but differently oriented.[21,22]

2. Materials and Methods

2.1. Sample Preparation. OtCPF1 and OtCPF2 were overexpressed in *E. coli* as glutathione S-transferase (GST) fusion proteins. The expression and purification protocols have already been described for OtCPF1[35] and were also used for OtCPF2. Briefly, purification was made on a gluthatione Sepharose 4B resin (Amersham Biosciences) which binds the GST tag. The proteins were released by adding a GSH (reduced L-gluthatione) rich elution buffer (Tris HCl pH 8.0 100 mmol L^{-1}, NaCl 100 mmol L^{-1}, GSH 20 mmol L^{-1}). We have shown in ref 35 that the presence of GSH in OtCPF1 samples induces large changes of the chromophore composition under continuous irradiation. Such an effect was not observed for OtCPF2 (see section 3.1). GSH, was therefore removed from OtCPF1, but not OtCPF2, samples by dialysis on a Cellu Sep T2 (6−8 kDa) membrane. The dialysis buffer contained: Tris HCl pH 8.0, 100 mmol L^{-1}, and NaCl 100 mmol L^{-1}. It was changed four times, every 30 min (the volume ratio of each step was 600). The purified proteins were concentrated by means of Microcon centrifugable membrane filters (10 kDa cutoff) in order to obtain a final volume of 50 μL. The concentrated samples reached a maximal absorbance (over 1-mm optical path) of: 0.04 at 448 nm for OtCPF1 and 0.07−0.18 at 386 nm for OtCPF2. After addition of glycerol (10% vol/vol), they were stored at−80 °C. Before each experiment, the samples were thawed at 0 °C, then centrifuged for 10 min at 14,000 rpm (15500*g*), at 5 °C, in order to remove aggregated proteins.

The denatured sample of OtCPF2 was obtained by heating the native protein at 65 °C for 10 min. Treatment of OtCPF2 with sodium borohydride was performed at 0 °C by adding freshly prepared 100 mmol L^{-1} solution of sodium borohydride (purchased from Merck) in Tris buffer.

2.2. Steady-State Spectroscopy and Photolysis. UV−vis absorption spectra were recorded with double-beam UV spectrophotometers: UV-mc^2 (Safas) or Cary 300 (Varian). Fluorescence spectra were measured with a fully corrected Fluoromax-3 (Jobin Yvon) spectrofluorometer. For steady-state photolysis, the sample contained in a 2 × 10 mm cuvette was irradiated either at 400 or 470 nm by the spectrofluorometer excitation beam. Measurements on the chromophore released in the solution after heat denaturation were done at room temperature. For all other experiments, the cell was thermostatted at 5 °C by a temperature-controlled bath (Minichiller Inox, Huber).

The cofactor composition of the sample was determined as previously detailed[35] by fitting the absorption spectrum of the protein to a sum of reference spectra of the pure components (namely FAD$_{ox}$, FADH[•], FADH$^-$ and, in the case of OtCPF2, MTHF). The apoprotein concentration, yielding the apoprotein/FAD ratio, was assessed both by measurement of the mass of precipitated apoprotein upon heat denaturation and measurement of the UV absorbance at 280 nm.[35] We give here the average of the (close) values found by the two measurements.

2.3. Time-Resolved Absorption Spectroscopy. Broadband (350−750 nm) femtosecond transient absorption spectra were recorded by the pump−probe with white-light continuum technique. The laser source is a commercial amplified Ti:Sapphire laser system (Tsunami+Spitfire, Spectra Physics) delivering 50-fs pulses at 775 nm, at 1 kHz repetition rate. The 470-nm pump beam (55 fs) was generated by using a two-stage noncollinear optical parametric amplifier (NOPA, Clark-MXR). The energy used to excite the samples ranged from 230 to 330 nJ per pulse, focused on a diameter of about 80 μm. Care was taken to check that this fluence lay in

the linear regime. The continuum probe beam was generated by focusing a few μJ/pulse of the 775-nm beam on a moving CaF$_2$ plate and split into a sample beam and a reference beam. The pump and probe beams were focused by 90° off-axis parabolic mirrors onto the sample cell and crossed at an angle of ca. 5°. The diameter of the pump beam slightly exceeded that of the probe beam. The probe beam was delayed with respect to the pump beam by a motorized optical delay line. The sample solutions were contained in 2-mm-wide, 1-mm-thick, fused-silica cuvettes, thermostatted at 5 °C to prevent protein degradation. The cuvette holder was continuously moved up and down (one dimension) in order to avoid photolysis, at a maximum speed of 20 mm/sec (which guarantees at displacement of 120 μm between each pump shot); the oscillation frequency was about 0.4 Hz. The experiments were stopped before any substantial degradation of the sample, inducing scattering of the probe beam, became visible (the steady-state absorbance of the samples was continuously monitored during the experiments). The probe beams (reference and sample) were then dispersed in a spectrograph (Acton SP306i) and recorded at 333 Hz on a CCD camera (Roper Scientific, Spec-10 100B, 100 × 1340 pixels); 6000 to 24000 pump shots were averaged to obtain the differential absorbance (ΔA) spectra. For isotropic conditions, the linear polarizations of the pump and probe beams were set at the magic angle (54.7°). For anisotropic conditions, they were set at 45°, and analyzers were inserted after the sample to alternatively record the parallel and perpendicular contributions.

The ΔA spectra were corrected from the chirp of the probe beam—independently measured by recording cross-phase modulation in the pure solvent. Scattering of the pump beam was removed of the differential spectra, both for data analysis and figure presentation.

2.4. Data Analysis. The transient absorption data were globally fitted to a sum of exponential functions, convoluted by a Gaussian function representing the setup response function, after dimensional reduction and noise filtering (see all technical details in ref 36) by singular value decomposition (SVD).[37] The number of retained singular values at the stage of analysis of the truncated data matrix (where times below ∼200 fs were removed in order to get rid of a of a cross-phase modulation artifact during pump−probe overlap) was four, which was enough to ensure that no information loss could alter the subsequent global fitting procedure. The decay-associated difference spectrum (DADS, i.e. spectrum of preexponential factors) of each time component was calculated over the entire experimental spectral range. This description allowed us to calculate the differential spectra associated to the species (species-associated difference spectra, SADS) of simple kinetic models.[38] For a sequential scheme with 100% conversion yield from one species to the next and increasing lifetimes, SADS are named evolution-associated difference spectra (EADS).[39] The EADS provide a dynamically meaningful abstract of the experimental data, which benefits both from deconvolution of the response function (EADS1 is the differential spectrum of initial excited state, extrapolated at $t = 0$) and SVD noise reduction.

2.5. Homology Modeling. The sequences of the OtCPF1 and OtCPF2 genes were aligned on other CPF genes, and homology models were subsequently generated by optimizing the tertiary structure of the proteins on the basis of proper templates. Details on the methods used for this work are given in Supporting Information (section 8).

(36) Brazard, J.; Ley, C.; Lacombat, F.; Plaza, P.; Martin, M. M.; Checcucci, G.; Lenci, F. *J. Phys. Chem. B* **2008**, *112*, 15182–15194.
(37) Henry, E. R.; Hofrichter, J. *Methods Enzymol.* **1992**, *210*, 129–193.
(38) Ernsting, N. P.; Kovalenko, S. A.; Senyushkina, T.; Saam, J.; Farztdinov, V. *J. Phys. Chem. A* **2001**, *105*, 3443–3453.
(39) van Stokkum, I. H. M.; Delmar, S. L.; van Grondelle, R. *Biochim. Biophys. Acta Bioenerg.* **2004**, *1657*, 82–104.
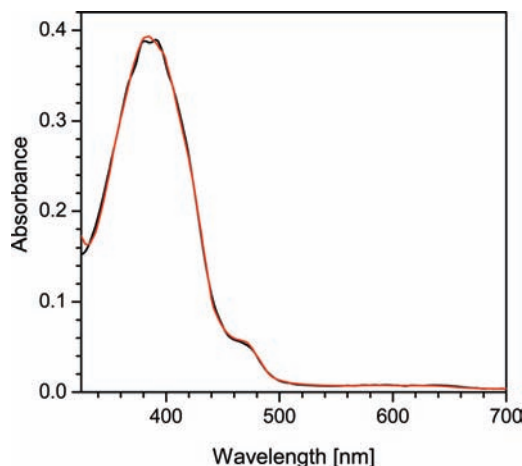
Figure 2. Steady-state absorption spectrum of OtCPF2 in Tris buffer (black) and the corresponding best fit (red) obtained with a weighted sum of the spectra of FAD_{ox}, $FADH^{\bullet}$, $FADH^{-}$ and MTHF bound in *E. coli* CPD photolyase.[41]

3. Results

In the following subsections, we first report the steady-state absorption and fluorescence spectroscopy of OtCPF2 allowing the quantitative analysis of its FAD and MTHF chromophore content. We then present the study of the primary events following excitation of FAD_{ox} in both OtCPF1 and OtCPF2, by femtosecond isotropic broadband absorption spectroscopy. We finally report a study of OtCPF2 by femtosecond polarized absorption spectroscopy.

3.1. Cofactor Content of OtCPF1 and OtCPF2. As mentioned in the Introduction, the steady-state spectroscopic properties of OtCPF1 were previously published.[35] After purification, its only noncovalently bound cofactor is FAD, mainly found in the oxidized form (FAD_{ox}), absorbing around 366 and 448 nm. The absorption spectrum of OtCPF2 is more complex (Figure 2). It consists of a major band centered at 386 nm, a weak band at 470 nm and a minor band extending from 500 to 675 nm. The intense peak at 386 nm shows the presence of enzyme-bound MTHF,[4,40] and the small bands between 450 and 700 nm indicate the coexistence of flavins in oxidized and neutral semiquinone states.[41] The presence of fully reduced flavin cannot be excluded because this state significantly absorbs between 320 and 450 nm, although with a lower molar extinction coefficient than MTHF.[42]

Further chemical tests evidenced the presence of MTHF and FAD in OtCPF2 (see details in Supporting Information, section 1). The fluorescence spectrum of OtCPF2 shows a peak at 493 nm mainly due to MTHF. This peak disappears upon reacting the protein with sodium borohydride, which is characteristic of the presence of MTHF.[43] Moreover, the fluorescence of the flavin released from the protein upon heat denaturation shows a peak at 525 nm. This typical emission of fully oxidized flavin shows a 5-fold intensity increase upon lowering the pH from 8.0 to 3.0. This effect, which is not observed for flavin

mononucleotide or riboflavin, clearly characterizes FAD. It is due to the protonation of the adenine at pH 3.0 and the subsequent opening of the stacked intramolecular complex which partly quenches the fluorescence of the isoalloxazine at pH 8.0.[44,45] It is therefore established that the flavin noncovalently bound to OtCPF2 is FAD.

As mentioned above, FAD is likely found in three redox states (FAD_{ox}, $FADH^{\bullet}$ and $FADH^{-}$) in OtCPF2. As previously described for OtCPF1,[35] we confirmed this hypothesis by globally fitting the absorption spectrum of our OtCPF2 samples with a weighted sum of the absorption coefficient spectra of FAD_{ox}, $FADH^{\bullet}$, $FADH^{-}$ and, in the present case, of MTHF. The best fit was obtained by using published spectra of these species bound to *E. coli* CPD photolyase.[41] The good quality of the fit (see Figure 2, red line) indicates there is no other chromophore, absorbing in the UV−vis domain, bound to OtCPF2. For a freshly thawed diluted sample the resulting concentrations were: $[FAD_{ox}] = 7.7 \pm 0.1$ μmol L^{-1} (26% of total FAD content), $[FADH^{\bullet}] = 2.6 \pm 0.2$ μmol L^{-1} (9%), $[FADH^{-}] = 18.7 \pm 0.3$ μmol L^{-1} (65%) and $[MTHF] = 19.05 \pm 0.05$ μmol L^{-1}. The total concentration of FAD and the concentration of MTHF were also calculated by a global fit of the absorption spectrum of the supernatant obtained after heat denaturation of OtCPF2 (see Supporting Information, section 2) and were found in very good agreement with the present results. We retained the average values, i.e.: $[FAD] = 28.5 \pm 0.7$ μmol L^{-1} and $[MTHF] = 19.8 \pm 0.3$ μmol L^{-1}. It appears that MTHF is in substoichiometric ratio (0.69) relative to FAD, which had already been observed for other CPF proteins.[1]

The presence of FAD_{ox} and $FADH^{\bullet}$ in purified OtCPF2 samples is likely due to the oxidation of $FADH^{-}$ during purification and storage of the proteins under aerobic conditions. The mixture of FAD redox states may not reflect a physiological function of OtCPF2. The predominance of $FADH^{-}$ in purified OtCPF2, as opposed to purified OtCPF1, may indicate that FAD is mainly in its fully reduced form *in vivo* and/or that the chromophore is less exposed to air in OtCPF2 than in OtCPF1.

The apoprotein concentration of OtCPF2 was found to be 39 $\pm$ 8 μmol L^{-1}. The FAD/apoprotein and MTHF/apoprotein ratios are 73% and 51%, respectively. These substoichiometric ratios were already reported in the literature for other purified CPF proteins.[1]

Contrary to OtCPF1,[35] OtCPF2 samples are photochemically stable at 5 °C, upon continuous irradiation at 400 and 470 nm, even without removing GSH. We interpret this stability by assuming that the slow electron recombination reaction occurring after photoreduction of FAD is, in OtCPF2, faster than the reduction of the oxidized protein residue, i.e. the distal WH_d radical if the Brettel−Vos mechanism applies, by reduced glutathione. This radical may as well be less exposed to the solvent in OtCPF2 than in OtCPF1.

3.2. Isotropic Transient Absorption Spectroscopy of OtCPF1. The absorbance of the OtCPF1-dialyzed sample chosen for transient absorption spectroscopy was 0.04 at 448 nm. The corresponding distribution of ground-state species was: 66% FAD_{ox}, 7% $FADH^{\bullet}$ and 27% $FADH^{-}$. After excitation of dialyzed OtCPF1 with 55 fs pulses at 470 nm, the initial excited-state fractions (x_i^*; the star indicates the excited state) were calculated to be 88% FAD_{ox}^*, 5% $FADH^{\bullet *}$ and 7% $FADH^{-*}$, by using the following formula (for each species *i*):

(40) Worthington, E. N.; Kavakli, I. H.; Berrocal-Tito, G.; Bondo, B. E.; Sancar, A. *J. Biol. Chem.* **2003**, *278*, 39143–39154.
(41) Jorns, M. S.; Wang, B. Y.; Jordan, S. P.; Chanderkar, L. P. *Biochemistry.* **1990**, *29*, 552–561.
(42) Song, S. H.; Dick, B.; Penzkofer, A.; Pokorny, R.; Batschauer, A.; Essen, L. O. *J. Photochem. Photobiol. B* **2006**, *85*, 1–16.
(43) Hamm-Alvarez, S.; Sancar, A.; Rajagopalan, K. V. *J. Biol. Chem.* **1989**, *264*, 9649–9656.

(44) Faeder, E. J.; Siegel, L. M. *Anal. Biochem.* **1973**, *53*, 332–336.
(45) Barrio, J. R.; Tolman, G. L.; Leonard, N. J.; Spencer, R. D.; Weber, G. *Proc. Natl. Acad. Sci. U.S.A.* **1973**, *70*, 941–943.

$$\chi_i^* = \frac{c_i \times \varepsilon_{470}(i)}{\sum\limits_i c_i \times \varepsilon_{470}(i)} \qquad (1)$$

where c_i is the ground-state concentration of species i and $\varepsilon_{470}(i)$ is the molar extinction coefficient of species i, averaged between 460 and 480 nm in order to account for the broad spectral width of the excitation pulse.

Although the initial excited population is a mixture of states, it mainly contains excited FAD_{ox}. It is worth noting that, contrary to our previous steady-state photolysis findings,[35] no accumulation of any photoproduct was detected during the present experiments. This is due to the dialysis of the OtCPF1 sample which efficiently removed GSH.

Figure 3 presents an overview of transient absorption spectra of OtCPF1 after excitation at 470 nm, for pump−probe delays ranging between 0.2 and 1400 ps. At 0.2 ps delay (Figure 3A) one observes three positive ΔA bands that are dominated by transient absorption contributions: a large one starting below 416 nm, a small one centered around 508 nm, and a broad structure extending beyond 580 nm. Ground-state bleaching is clearly seen around 447 nm and gives rise to a net negative band between 416 nm and about 490 nm, where it is dominant. Stimulated emission is apparent around 540 nm although superimposed to a transient-absorption background. Stimulated emission is dominant and produces a net negative peak, between 527 and 580 nm only.

The general shape of this differential spectrum is fully compatible with the excitation of FAD_{ox} essentially. The difference with transient spectra of oxidized FAD[46] or riboflavin[47] in solution mostly lies in the position of the stimulated-emission band, which is blue-shifted in the case of OtCPF1. This effect is likely due to the lower polarity of the FAD binding pocket, as compared to bulk water. The temporal evolution of the spectra shows three phases:

- Phase 1 (Figure 3A): The blue positive band and the bleaching band remain stable between 0.2 and 1 ps. The stimulated emission contribution, however, disappears and leaves a positive band, a maximum of which is seen around 590 nm. A nontrivial ($\Delta A \neq 0$) temporary isosbestic point is seen at 655 nm.
- Phase 2 (Figure 3B): Between 1 and 20 ps, one notes a weak quasi-proportional (homothetic) decay of all the bands except for the transient absorption one at 493−527 nm, which decays slightly more steeply.
- Phase 3 (Figure 3C): All bands decay slowly and quasi-proportionally between 20 and 1400 ps.

Figure 3A, demonstrates that a photoinduced reaction occurs between 0.2 and 1 ps. The disappearance of stimulated emission, but not of ground-state bleaching, shows that FAD_{ox} undergoes prompt de-excitation and concomitantly produces new photoproducts responsible for the subsequent transient absorption changes. This scheme is in good agreement with the nontrivial temporary isosbestic point observed at 655 nm. The fact that nearly no ground-state recovery occurs indicates that this early reaction has a very high yield. According to our previous observation of a photoreduction of FAD_{ox} under continuous irradiation,[35] the present reaction is likely to be assigned to the primary reduction of excited FAD_{ox}. The literature on the
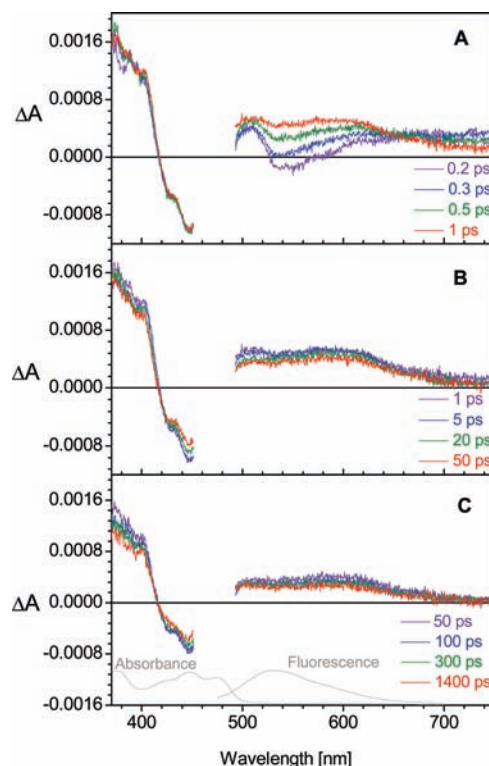

Figure 3. Transient absorption spectra of OtCPF1 in Tris buffer after excitation at 470 nm and under isotropic conditions (magic angle). The time evolution of the spectra between 0.2 and 1 ps is displayed in A, between 1 and 50 ps in B, and between 40 and 1400 ps in C. The steady-state absorption and fluorescence spectra of OtCPF1 are recalled in gray lines in C.

photoactivation of FAD inside of CPF proteins,[16–23] and other flavoproteins,[26–31,48] points to the involvement of a proximal aromatic amino acid, tryptophan or tyrosine, as the electron donor. The analysis of the spectra after 1 ps pump−probe delay will allow a precise determination of this donor (see Discussion, section 4.1.1). In the meantime note that partial ground-state recovery is seen after 1 ps delay, accompanied by a few spectral modifications of the photoproducts, and that a long-lived residual photoproduct spectrum is still observed at 1.4 ns.

Global analysis of the data was performed with best results by using three exponential components plus a plateau. The lifetimes of the exponentials were found to be: 0.39 ± 0.03 ps, 9 ± 2 ps and 81 ± 8 ps. The corresponding DADS (pre-exponential factor spectra) are given and commented in Supporting Information (section 3). The EADS (see definition in section 2.4) are provided as well.

3.3. Isotropic Transient Absorption Spectroscopy of OtCPF2. The OtCPF2 sample used for isotropic transient absorption spectroscopy is called OtCPF2-Iso. Its ground-state chromophore distribution is the following: 16% FAD_{ox}, 2% FADH·, 36% $FADH^-$, and 46% MTHF. After excitation at 470 nm (55 fs pulses), the distribution of the initial excited states is expected to be the following: 78% FAD_{ox}^*, 5% FADH·*, 10% $FADH^{-*}$, and 7% MTHF*. The main excited species is FAD_{ox}.

The transient absorption spectrum of OtCPF2-Iso at 0.25 ps (Figure 4A) pump−probe delay is very similar to the one of OtCPF1 at 0.2 ps, with characteristic features of excited FAD_{ox}.

(46) Li, G. F.; Glusac, K. D. *J. Phys. Chem. A* **2008**, *112*, 4573–4583.
(47) Weigel, A.; Dobryakov, A. L.; Veiga, M.; Lustres, J. L. P. *J. Phys. Chem. A* **2008**, *112*, 12054–12065.
(48) Pan, J.; Byrdin, M.; Aubert, C.; Eker, A. P. M.; Brettel, K.; Vos, M. H. *J. Phys. Chem. B* **2004**, *108*, 10160–10167.
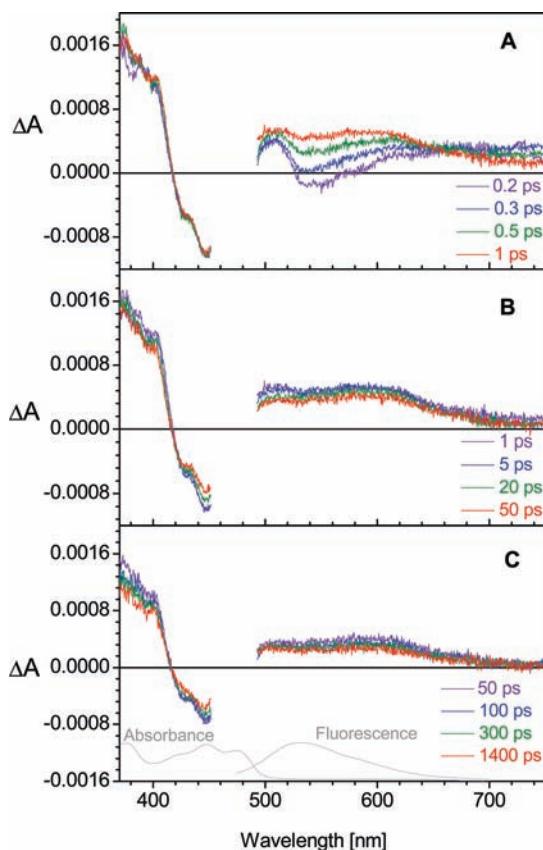
Figure 4. Transient absorption spectra of OtCPF2 in Tris buffer after excitation at 470 nm and under isotropic conditions (magic angle). The time evolution of the spectra between 0.25 and 1.5 ps is displayed in A, between 1.5 and 200 ps in B, and between 200 and 1400 ps in C. The steady-state absorption spectrum of FAD_{ox}[41] and fluorescence spectrum of OtCPF2 are recalled in gray lines in C.

The temporal evolution of spectra between 0.25 and 1400 ps is plotted in Figure 4. As for OtCPF1, it can be divided in three phases:

- Phase 1 (Figure 4A): the bleaching band (peaking at 442 nm) and the blue transient absorption band (below 415 nm) do not evolve for 0.25 to 1.5 ps pump−probe delays. During the same time, the stimulated-emission band (peaking around 540 nm) disappears and is replaced by a broad transient absorption band. A temporary isosbestic point is observed at 654 nm.
- Phase 2 (Figure 4B): a weak and quasi-proportional decay of all bands, including bleaching, is observed between 1.5 and 50 ps. The transient absorption band around 505 nm is seen to flatten slightly.
- Phase 3 (Figure 4C): little evolution of the spectra is seen from 200 to 1400 ps, except for a decrease of the visible transient absorption, around 600 nm.

A photoreaction obviously occurs between 0.25 and 1.5 ps, evidenced by the loss of stimulated emission, the simultaneous growth of a new transient absorption band and the presence of an isosbestic point at 654 nm. Almost no recovery of the ground state occurs in this period of time, since the bleaching band does not evolve. As previously seen for OtCPF1, photoreduction of excited FAD_{ox} is expected and the electron donor could be a nearby aromatic amino acid, a tryptophan or a tyrosine. After the initial photoreaction, a partial ground-state recovery is observed between 1.5 and 50 ps and a residual, apparently long-lived, spectrum remains at 1.4 ns.
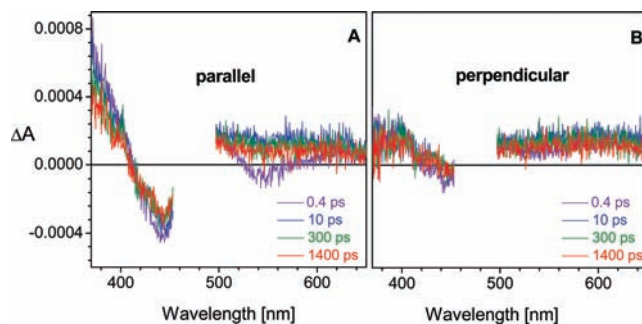
Figure 5. Transient absorption spectra of OtCPF2 in Tris buffer after excitation at 470 nm, with pump and probe beams polarized parallel (A) and perpendicular (B).

The data were globally fitted to a sum of three exponential components plus a plateau. The lifetimes of the exponentials were found to be: 0.59 ± 0.03 ps, 13 ± 3 ps and 340 ± 43 ps. The corresponding DADS and EADS are given in Supporting Information (section 4). Let us note for now that DADS2, attached to the 13-ps lifetime, presents a shallow dip around 540 nm which evokes the loss of a stimulated emission contribution.

3.4. Polarized Transient Absorption Spectroscopy of OtCPF2. We measured polarized transient absorption spectra of an OtCPF2 sample (called OtCPF2-Aniso), which happened to be more dilute than OtCPF-Iso. The initial excited-state population of OtCPF2-Aniso is mainly made of FAD_{ox}* (in fact: 64% FAD_{ox}*, 12% FADH•*, 16% FADH⁻* and 8% MTHF*).

Figure 5 compares the parallel ($\Delta A_{\parallel}$) and perpendicular ($\Delta A_{\perp}$) transient absorption spectra at four selected pump−probe delays (0.4 ps, 10 ps, 300 and 1400 ps). We observe that at each delay, $\Delta A_{\parallel}$ and $\Delta A_{\perp}$ are different in the bleaching and blue transient absorption bands. On the other hand, for a 400 fs pump−probe delay, $\Delta A_{\parallel}$ and $\Delta A_{\perp}$ do not overlap in the stimulated emission and red transient absorption bands but do overlap for the longer delays.

The validity of the polarized spectra was checked by reconstructing the isotropic spectra. We found that the rebuilt isotropic spectra are very similar to those directly measured for OtCPF2-Iso (see Supporting Information, section 5). Global analysis performed of those rebuilt spectra yielded time constants in good agreement with those found for the isotropic data (see section 3.3 and Supporting Information, section 5).

We next performed a simultaneous global analysis of the parallel and perpendicular data. The best fit was obtained with the same fit function as for the isotropic data, i.e. three exponentials plus a plateau. The exponential lifetimes were found to be 0.46 ± 0.05 ps, 9 ± 2 ps and 301 ± 50 ps, in close agreement with those found under isotropic conditions. It therefore appears that rotational diffusion does not play any role in our polarized measurements. This is explained by the rigid interaction between FAD and the protein, the rotational correlation time of which is expected to be larger than 30 ns,[21] hence not observable within our temporal observation window.

We further calculated the anisotropy. In order to improve the signal-to-noise (S/N) ratio, the above-mentioned global fit of rebuilt isotropic data was used to substitute the denominator in the anisotropy definition below (see details in ref 21):

$$r(t,\lambda) = \frac{\Delta A_{\parallel}(t,\lambda) - \Delta A_{\perp}(t,\lambda)}{\Delta A_{\parallel}(t,\lambda) + 2 \times \Delta A_{\perp}(t,\lambda)} \quad (2)$$
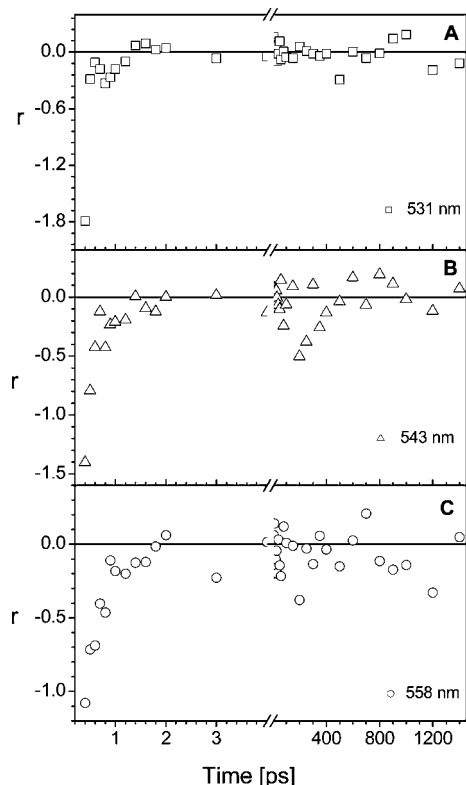
Figure 6. Anisotropy kinetics at 531 nm (squares, A), 543 nm (triangles, B), and 558 nm (circles, C) of OtCPF2 in Tris buffer, after excitation at 470 nm.

The anisotropy decay traces obtained in such a way are represented at several selected wavelengths in Figure 6. A strong anisotropy variation is observed within approximately the first picosecond, from 526 to 558 nm, as expected from the observations of Figure 5. This change is to be related to the primary photoreaction described in section 3.3. At longer pump−probe delays the S/N ratio of these anisotropy data is quite poor and does not allow any precise analysis. We will however propose in section 4.2.4 a noise-reduction method that tentatively allows to get more insight into the anisotropy behavior at long times.

4. Discussion

4.1. Photoactivation of FAD$_{ox}$ Bound to OtCPF1. 4.1.1. Identification of the Photoproducts. In order to determine the nature of the products yielded by the primary photoreaction of OtCPF1, occurring in 0.39 ps, we compared the experimental data to reconstructed difference spectra (i.e., including the bleaching of FAD$_{ox}$) of different putative photoproducts. As pointed out in section 3.2, the primary reaction is expected to be the reduction of excited FAD$_{ox}$. We previously showed that continuous irradiation of OtCPF1 induces reduction of FAD$_{ox}$ into FADH•.[35] The present ultrafast reaction might, however, simply yield FAD•−, this radical anion undergoing protonation in a longer time scale. We have seen in section 3.2 that the electron donor is likely a tryptophan or a tyrosine residue. During the 0.39-ps step, these aromatic amino-acids could simply be oxidized into tryptophanyl or tyrosyl radical cations (noted WH•+ and YOH•+, respectively). Alternatively, they could get deprotonated and turn into tryptophanyl or tyrosyl neutral radicals (W• and YO•, respectively). As the pK_a of radical tyrosyl
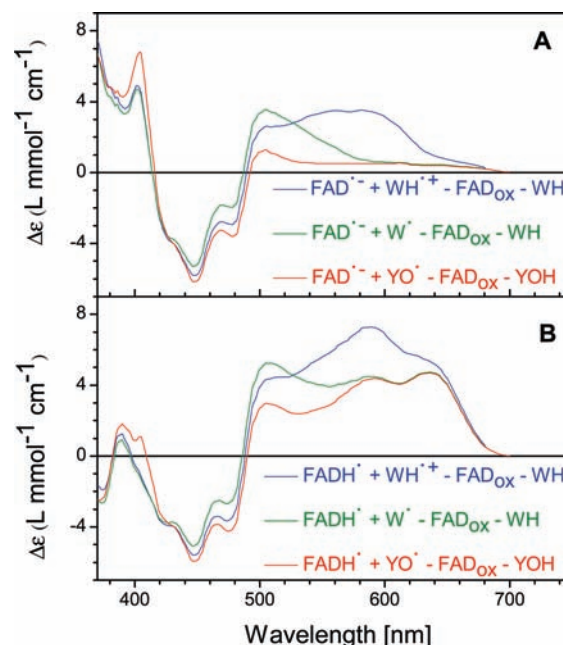

Figure 7. Reconstructed differential molar extinction coefficients spectra of putative photoproducts obtained after photoreduction of FAD$_{ox}$. The cases of FAD$_{ox}$ reduction into FAD•− and into FADH• are displayed in panels A and B, respectively. The spectra were built with published spectra of FAD$_{ox}$, FADH•,[53] FAD•−,[50] WH•+, W•[51] and YO•.[16]

lies below 0,[49] fast deprotonation of YOH•+ would, however, be very likely.

The reconstructed spectra displayed in Figure 7 were built with previously published absorption spectra of FAD•−,[50] WH•+, W•[51] and YO•.[16] YOH•+ was not considered because its absorption spectrum is currently not available in the literature. We did not take into account possible charge-transfer bands, such as those described for other flavoproteins by Miura,[52] arising from the close π interaction of the reduced and oxidized radicals. As shown in Figure 8 (section 4.1.2), the π system of the isoalloxazine ring is not close and parallel enough to the nearest electron donor to justify the presence of such additional bands.

It is clear from Figure 7B that the bleaching band of FAD$_{ox}$ below 390 nm is not dominated by the absorption of FADH• or other radicals and appears with a negative sign. On the other hand, Figure 7A shows that the absorption of FAD•− dominates the bleaching band of FAD$_{ox}$ below 390 nm and produces a net positive band in the UV. Since all the transient absorption spectra of OtCPF1 display a large positive band in UV, it must be concluded that FAD$_{ox}$ is not reduced to FADH• within our temporal observation window (limited to 1.4 ns).

Retaining the hypothesis of reduction of FAD$_{ox}$ into FAD•−, it is interesting to note that the experimental spectra recorded after 1 ps (Figure 3B) show a broad positive band between 493 and 750 nm, with a slope break beyond 630 nm. This observation leads us to exclude deprotonated tyrosyl and

(49) Gerken, S.; Brettel, K.; Schlodder, E.; Witt, H. T. *FEBS Lett.* **1988**, *237*, 69–75.
(50) Berndt, A.; Kottke, T.; Breitkreuz, H.; Dvorsky, R.; Hennig, S.; Alexander, M.; Wolf, E. *J. Biol. Chem.* **2007**, *282*, 13011–13021.
(51) Solar, S.; Getoff, N.; Surdhar, P. S.; Armstrong, D. A.; Singh, A. *J. Phys. Chem.* **1991**, *95*, 3639–3643.
(52) Miura, R. *Chem. Rec.* **2001**, *1*, 183–194.
(53) Schleicher, E.; Hitomi, K.; Kay, C. W. M.; Getzoff, E. D.; Todo, T.; Weber, S. *J. Biol. Chem.* **2007**, *282*, 4738–4747.
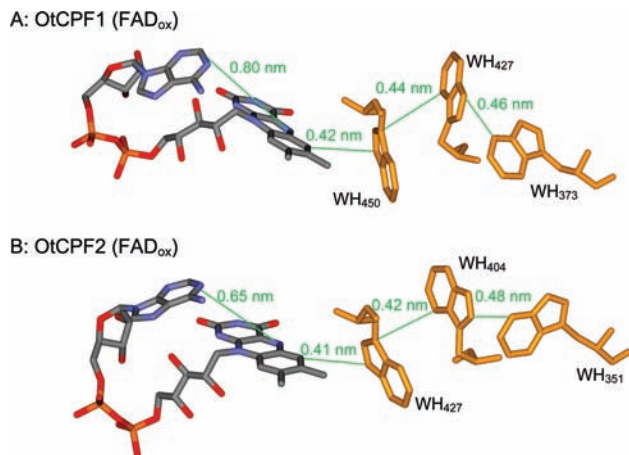
A: OtCPF1 (FAD$_{ox}$)

B: OtCPF2 (FAD$_{ox}$)

Figure 8. Tryptophan chain involved in the photoactivation of FAD$_{ox}$ inside OtCPF1 (A) and OtCPF2 (B) as calculated by homology modeling. The main relevant edge-to-edge distances are represented in green.

tryptophanyl radicals as possible photoproducts since they yield very small absorbance beyond 580 nm (Figure 7A). The best match between the reconstructed and experimental spectra therefore corresponds to the reduction of FAD$_{ox}$ into FAD$^{•-}$ and the oxidation of WH into WH$^{•+}$.

A comparison of the experimental transient absorption spectrum obtained after the reaction occurring in 390 fs and the reconstructed spectrum corresponding to FAD$^{•-}$ and WH$^{•+}$ is proposed in Supporting Information (section 7). The superposition is not perfect but the spectra bear a close resemblance. The mismatches could in part be due to our insufficient knowledge of the real spectra of the different radicals inside OtCPF1 and also to the fact that other species than FAD$_{ox}$ were excited in our experiment (5% FADH$^{•}$*, 7% FADH^{-}*) and may contribute to the data. Excited FADH^{-}, the lifetime of which is 1.7 ns in *E. coli* CPD photolyase, has a broad positive band from 450 to 900 nm[54] which could explain the presence of nonzero absorbance in the transient data beyond 580 nm. As far as excited FADH$^{•}$ is concerned, it presents two negative minima at 500 and 580 nm due to bleaching.[19] This species would also be expected to undergo photoreduction in the picosecond regime and give rise to FADH^{-} and WH$^{•+}$ photoproducts, characterized by a negative differential signal between 435 and 640 nm.[19] However, these spectral features are not recognizable in our OtCPF1 data.

As mentioned in section 3.2, the evolution of the transient absorption spectra of OtCPF1 after the first picosecond is roughly proportional (homothetic). The EADS presented in Supporting Information (section 3) more precisely demonstrate some moderate shape evolution during the 9 ps step (EADS2 and EADS3 are not exactly identical) and very little during the 81 ps step (EADS3 and EADS4 are very close). On this basis we propose that the photoproducts found along the evolution of the transient spectra following the initial photoreduction all correspond to the FAD$^{•-}$/WH$^{•+}$ pair. As proposed above, the spectral differences could be due to the contributions of the other excited species.

4.1.2. Kinetic Model. In order to explain the partial decay of the FAD$^{•-}$/WH$^{•+}$ product pair at each step of the multiexponential dynamics, it is necessary to invoke a partial charge recombination, restoring the initial FAD$_{ox}$ and WH molecules,

at each of those steps. The fact that this charge recombination is never complete (in our observed time scale) and the system is still evolving after the 9 ps or the 81 ps component means that another chemical reaction must compete with charge recombination, at each step. Since this reaction does not change the chemical nature of the species (FAD$^{•-}$ and WH$^{•+}$) we evoke the Brettel–Vos mechanism,[18–24] by which the primary oxidized tryptophan, located close to the flavin, is reduced by a more distant tryptophan, in turn reduced by a third tryptophan situated further away. This electron hopping mechanism is precisely what allows competing with fast electron recombination and stabilizing the FAD$^{•-}$/WH$^{•+}$ pair by increasing the distance between the radicals.

The kinetic model we propose for OtCPF1 therefore combines electron hopping along a tryptophan chain and electron recombination at each kinetic step. The protein alignment and homology modeling (see Supporting Information, section 8) we performed on the OtCPF1 sequence allowed us to show that the tryptophan chain involved in the photoactivation of FADH$^{•}$ into EcCPD (see Introduction) is well conserved within OtCPF1. Its calculated spatial placement, represented in Figure 8A, is in fact very similar to that of EcCPD.[55]

We therefore propose that, after excitation at 470 nm, FAD$_{ox}$ is reduced in 390 fs into FAD$^{•-}$ by WH$_{450}$. The WH$_{450}^{•+}$ radical is then reduced by WH$_{427}$, while electron recombination from FAD$^{•-}$ to WH$_{450}^{•+}$ occurs, in 9 ps. WH$_{427}^{•+}$ is finally reduced by WH$_{373}$ (exposed to the surface of the protein), while charge recombination between WH$_{427}^{•+}$ and FAD$^{•-}$ proceeds, in 81 ps. The final state accessible to our experiment is then made of FAD$^{•-}$ and WH$_{373}^{•+}$. This kinetic model is summarized in Figure 9A.

We further proceeded to an elementary target analysis of our data in order to estimate the rate constants attached to each process. The applied constraint (described in more detail in ref 56) consisted in imposing that all SADS exhibit approximately the same negative bleaching contribution around 440 nm. No ground-state recovery in competition with the first step was necessary. As far as steps 2 (9 ps) and 3 (81 ps) are concerned, the rate constants of electron transfer are noted k_2 and k_3, respectively, while the charge recombination rates are written k'_2 and k'_3, respectively. We obtained: $k_2 = 10^{11}$ s^{-1}, $k'_2 = 1.1 \times 10^{10}$ s^{-1}, $k_3 = 8 \times 10^9$ s^{-1} and $k'_3 = 4.3 \times 10^9$ s^{-1}. The corresponding SADS are shown in Figure 9B. These rate constants correspond to a yield of electron transfer of $\Phi_2 = 90\%$ during step 2 and $\Phi_3 = 65\%$ during step 3. Since the yield of primary photoreduction is 1 in our model, this means that the overall charge separation yield achieved in the presently observed time window is ∼59%.

4.2. Photoactivation of FAD$_{ox}$ Bound to OtCPF2. 4.2.1. Heterogeneity in the Ground State. The transient absorption spectra of OtCPF2 are qualitatively very similar to those of OtCPF1 (compare Figures 3 and 4). We noted in section 3.3, however, that the pre-exponential factor spectrum attached to the 13 ps component (DADS2) contains a signature of FAD$_{ox}$ excited-state decay (see Supporting Information, section 4). This means that a slight contribution of stimulated emission is still recognizable during the 13 ps step of OtCPF2 while no such stimulated emission was seen during the 9 ps step of OtCPF1.

(54) Okamura, T.; Sancar, A.; Heelis, P. F.; Begley, T. P.; Hirata, Y.; Mataga, N. *J. Am. Chem. Soc.* **1991**, *113*, 3143–3145.

(55) Park, H. W.; Kim, S. T.; Sancar, A.; Deisenhofer, J. *Science* **1995**, *268*, 1866–1872.

(56) Plaza, P.; Mahet, M.; Martin, M. M.; Checcucci, G.; Lenci, F. *J. Phys. Chem. B* **2007**, *111*, 690–696.
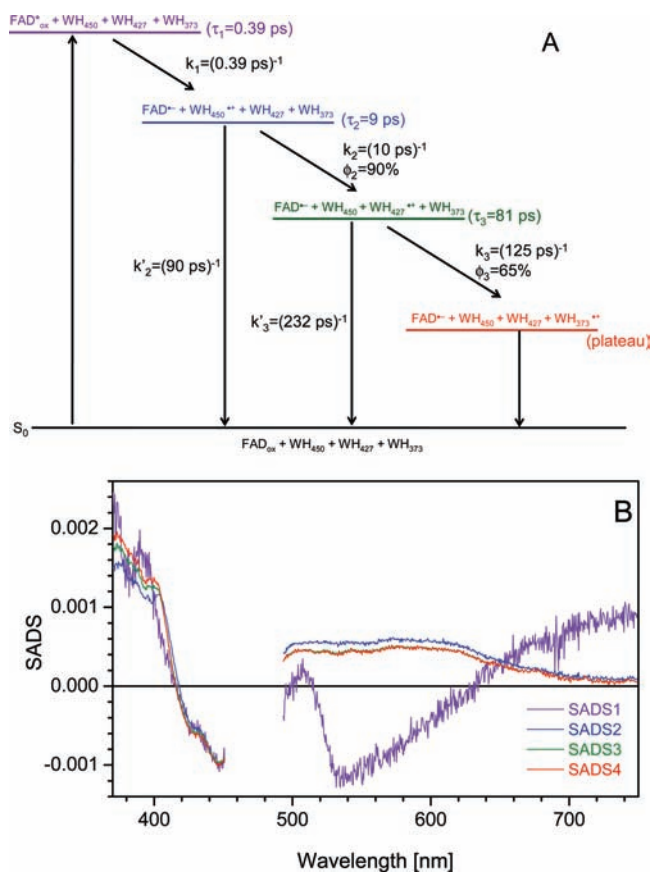
Figure 9. (A) Kinetic model proposed to describe the photoactivation of FAD_{ox} in OtCPF1. (B) Species-associated difference spectra (SADS) obtained by using the kinetic model described in A.

A discussion of this observation is provided in Supporting Information (section 9). We propose that our OtCPF2 sample is actually heterogeneous and contains two classes of FAD_{ox} populations. The main, so-called reactive, population is thought to give photoproducts in 0.59 ps, in a way very similar to that of OtCPF1. A secondary, so-called nonreactive population, would not undergo photoreduction but rather decay to the ground state in 13 ps, just as the closed conformation of FAD_{ox} does in solution (with 5−20 ps lifetime).[46,57−61] We tentatively propose that nonreactive FAD_{ox} could be bound to OtCPF2 in the binding site of MTHF, which is left free in 49% of the proteins in our purified samples (see section 3.1). The nonreactive population would contribute to DADS2 only; which does not exclude that the reactive population could also contribute to it. In this latter case, the fact that both populations share a common lifetime should be considered as a coincidence or a global analysis artifact. In what follows we will tentatively maintain the possibility that both reactive and nonreactive populations contribute to DADS2.

4.2.2. Identification of the Photoproducts. The primary photoreaction of (reactive) excited FAD_{ox} within OtCPF2 occurs

(57) Chosrowjan, H.; Taniguchi, S.; Mataga, N.; Tanaka, F.; Visser, A. *Chem. Phys. Lett.* **2003**, *378*, 354–358.
(58) Kao, Y. T.; Saxena, C.; He, T. F.; Guo, L. J.; Wang, L. J.; Sancar, A.; Zhong, D. P. *J. Am. Chem. Soc.* **2008**, *130*, 13132–13139.
(59) Kondo, M.; Nappa, J.; Ronayne, K. L.; Stelling, A. L.; Tonge, P. J.; Meech, S. R. *J. Phys. Chem. B* **2006**, *110*, 20107–20110.
(60) Stanley, R. J.; MacFarlane, A. W., Jr. *J. Phys. Chem. A* **2000**, *104*, 6899–6906.
(61) van den Berg, P. A. W.; Feenstra, K. A.; Mark, A. E.; Berendsen, H. J. C.; Visser, A. *J. Phys. Chem. B* **2002**, *106*, 8858–8869.
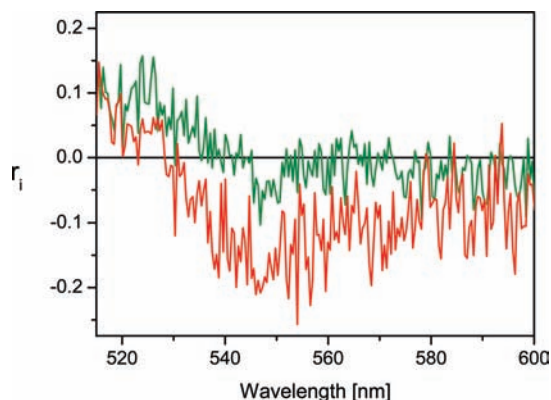
with a lifetime of 590 fs. Identifying the photoproducts just after this step (EADS2 in terms of evolution-associated difference spectra; see Supporting Information, section 4) is not straightforward because, as described above (section 4.2.1), the 13 ps component (DADS2) is likely to be assigned to a mixture of processes belonging to the reactive and nonreactive FAD_{ox} populations. We therefore focused on the transient absorption spectra left after the first two kinetic steps (EADS3 and EADS4).

We followed the same procedure as for OtCPF1 and compared these experimental spectra to reconstructed difference spectra of various photoreduction products. The only difference was that the FAD_{ox} and $FADH^\bullet$ spectra came from ref 41. As the transient absorption spectra of OtCPF2 and OtCPF1 are quite similar, it is not surprising that the best match corresponds to the $FAD^{\bullet-}/WH^{\bullet+}$ pair. This assignment is illustrated by the overlap of the reconstructed spectrum of $FAD^{\bullet-}/WH^{\bullet+}$ and of EADS3 presented in Supporting Information (section 10). The superposition is not perfect, but as mentioned for OtCPF1, the differences might be due to the contribution of other excited species (5% $FADH^{\bullet*}$, 10% $FADH^{-*}$ and 7% MTHF*) or to the unknown spectra of these species in OtCPF1.

4.2.3. Kinetic Model. The kinetic model we propose for the reactive population of OtCPF2 is essentially identical to the one of OtCPF1 (Figure 9A) and follows the Brettel−Vos mechanism.[18–23] By protein alignment we verified that the chain of three tryptophan residues is conserved in OtCPF2. These residues are identified as follows: WH_{427}, WH_{404} and WH_{351}, from the nearest to the most distant to FAD. Figure 8B shows their spatial disposition, as calculated by homology modeling.

The case of OtCPF2 is more complex than that of OtCPF1 because we identified in DADS2 (OtCPF2) a contribution coming from the nonreactive FAD_{ox} population (see section 4.2.1). It is thus not certain that the 13 ps step can be assigned to the reactive population. However, if it were the case (just as the 9 ps step of OtCPF1 belongs to the same chronologic process), the scheme would be that the excitation of FAD_{ox} leads to its reduction into $FAD^{\bullet-}$ by WH_{427} in 590 fs. $WH_{427}^{\bullet+}$ would then be reduced by WH_{404}, with concomitant partial charge recombination between $FAD^{\bullet-}$ and $WH_{427}^{\bullet+}$, in 13 ps. The last step would be the reduction of $WH_{404}^{\bullet+}$ by WH_{351}, accompanied by partial charge recombination between $FAD^{\bullet-}$ and $WH_{404}^{\bullet+}$, in 340 ps. The long-lived photoproducts would be $FAD^{\bullet-}$ and $WH_{351}^{\bullet+}$. We stress that this proposal should be considered with care, due to the above-mentioned uncertainties regarding the interpretation of DADS2. On the basis of our preliminary anisotropy data, a different tentative scenario will be devised in section 4.2.4. This is why we could not perform any reliable target analysis on the full OtCPF2 data. However, if we restrict the analysis to the last step (340 ps), we calculate an electron transfer yield of 77%. By excluding DADS2 from the dynamics (this approximation may not be too crude because DADS2 has a small amplitude), the primary photoreduction yield would only be 84%, which means that, contrary to OtCPF1, ground-state recovery probably competes with the ultrafast photoreduction reaction. The mechanism underlying this effect might be due to the interaction of the isoalloxazine and adenine moieties within the U-shaped conformation of FAD (see Figure 8B) characterizing CPF proteins.[1]

4.2.4. Anisotropy. We have seen in section 3.4 that the polarized transient absorption spectra of OtCPF2 could be simultaneously fitted to a sum of identical exponentials. This global analysis could then be used to produce parallel and perpendicular EADS, i.e. difference spectra of the species

Figure 10. Intrinsic anisotropy spectra associated to the EADS3 (green) and EADS4 (red) of OtCPF2, after excitation at 470 nm.

associated to a simple sequential kinetic model, with 100% conversion yield from one species to the next.

The particular interest of this treatment lies in a significant noise reduction of the polarized EADS (provided in Supporting Information, section 6), due to the SVD treatment, as compared to the corresponding raw transient spectra (section 3.4, Figure 5). This advantage allows calculating intrinsic (time-independent) anisotropies attached to each of those EADS, as follows:

$$r_{EADS} = \frac{EADS_{\parallel} - EADS_{\perp}}{EADS_{\parallel} + 2 \times EADS_{\perp}} \quad (3)$$

These ratios show a better S/N ratio than those which would be obtained with the raw spectra because they benefit from noise reduction, both in the numerator and denominator. They should however be considered as tentative since they heavily rely on the data analysis procedure. It is important to note that the difference spectra (SADS) associated to any kinetic model derived from the sequential one by adding ground-state recovery channels from the transient species, would be strictly proportional to the EADS. This means that the intrinsic anisotropies of the corresponding SADS would be equal to the above r_{EADS}. The r_{EADS} have thus a somewhat general validity, applicable to the model of Figure 9A for instance.

Since the interpretation of the 13-ps step of OtCPF2 is still uncertain, we only calculated the intrinsic anisotropies associated to EADS3 and EADS4 (named r_3 and r_4), i.e. after decay of the species evolving within the first two time components. They are represented in Figure 10 in the 515−600 nm spectral range. As the system evolves from state 3 (EADS3) to state 4 (EADS4) in 301 ps (and remains in state 4 within our temporal observation window), its anisotropy shifts from r_3 to r_4.

As pointed out by Byrdin et al.,[21] when a single transition is excited and a single transition is detected, the observed anisotropy depends on the angle β between the two transition dipole moments, according to:

$$r = \frac{3\cos^2\beta - 1}{5} \quad (4)$$

Since the only expected contribution to the transient absorption spectra around 550 nm, in the subnanosecond regime, comes from the tryptophanyl radical cation,[17] we can apply eq 4. Observing that $r_3 = 0 \pm 0.04$ and $r_4 = -0.15 \pm 0.07$ around 550 nm, we deduce $\beta_3 = 55° \pm 4°$ and $\beta_4 = 73° \pm 12°$ (the errors have been estimated from the noise levels in Figure 10). Although one must consider these numbers (affected by large

errors) with care because of the poor S/N ratio of the original data, this angle change is in favor of the Brettel−Vos mechanism of electron hopping along a chain of identical but differently oriented tryptophan residues.

We used our homology model of OtCPF2 to calculate the angles between transition dipole moments of FAD_{ox} and the three tryptophanyl radicals. We found 47°, 28° and 70° for $WH_{427}{}^{\bullet+}$ (proximal tryptophan), $WH_{404}{}^{\bullet+}$ (medium) and $WH_{351}{}^{\bullet+}$ (distal), respectively. We note that β_4 is close to the value corresponding to $WH_{351}{}^{\bullet+}$. With the same caution as above, we would deduce that the long-lived species appearing in our experimental data correspond to the $FAD^{\bullet-}/WH_{351}{}^{\bullet+}$ pair, as postulated in section 4.2.3. Along the same line, the value of β_3 might tentatively be identified with the expected angle for $WH_{427}{}^{\bullet+}$. In that case one would have to conclude differently from section 4.2.3 and hypothesize that the species decaying in about 300 ps is not $WH_{404}{}^{\bullet+}$ but $WH_{427}{}^{\bullet+}$, giving rise to $WH_{351}{}^{\bullet+}$ without observable intermediate. Such a situation would still be compatible with the hopping mechanism along the tryptophan triad as long as the rate for reduction of $WH_{404}{}^{\bullet+}$ (medium) by WH_{351} (distal) is much larger than the rate for reduction of $WH_{427}{}^{\bullet+}$ (proximal) by WH_{404} (medium). As a corollary, the kinetic component of 13 ps should then be entirely assigned to the putative nonreactive species introduced in section 4.2.1.

Again, the above discussion should be taken with care because of the large uncertainties related to the use of strongly noise-corrected spectra and predictions based on homology modeling.

4.3. Comparison with other CPF Proteins. We found that the primary photoreduction of excited FAD_{ox} in OtCPF1 and OtCPF2 (390 and 590 fs respectively) is, as expected (see Introduction), much faster than that of $FADH^{\bullet}$ in EcCPD (30 ps).[18−24] Our observation is in good agreement with the data of Kao et al. (0.5 to 1.8 ps) regarding the photoreduction of FAD_{ox} in several CPF proteins.[25] The faster photoreduction of FAD_{ox} can be explained by the fact that FAD_{ox} is a better oxidant than $FADH^{\bullet}$, which provides a larger driving force to the photoreduction reaction, and hence determines a faster reaction in the Marcus normal region.[62] Kao et al. indeed report a difference of driving force, $\Delta\Delta G$ ($FADH^{\bullet}$-FAD_{ox}), of about 0.44 eV for the photoreduction of FAD in EcCPD,[25] while Pan et al. report a $\Delta\Delta G$ ($FMNH^{\bullet}$-FMN_{ox}) of ∼0.7 eV in the context of the photoreduction of FMN in flavodoxin.[48] It is interesting to note that the reaction (FAD_{ox} photoreduction) is faster in OtCPF1 (390 fs) and OtCPF2 (590 fs) than in EcCPD (0.8−1.2 ps).[25] The distance between the flavin and the proximal tryptophan (judged from crystallographic measurements for EcCPD[55] and homology modeling for our proteins) however looks nearly identical for these three proteins. The difference could then be due to differences in the orientation and/or local chemical environment (finely tuning the oxidation potential) of the tryptophan residues. A simple check of the compatibility of these rates with the distance between the flavin and the proximal tryptophan residue can be done by using the "Moser−Dutton ruler",[63] which semiempirically relates the electron transfer rate k in proteins to the edge-to-edge distance R between partners (in Å), the reaction free energy ΔG and the reorganization energy λ (both in eV):

(62) Marcus, R. A.; Sutin, N. *Biochim. Biophys. Acta* **1985**, *811*, 265–322.
(63) Page, C. C.; Moser, C. C.; Chen, X. X.; Dutton, P. L. *Nature* **1999**, *402*, 47–52.

$$\log_{10} k = 15 - 0.6R - 3.1(\Delta G + \lambda)^2/\lambda \qquad (5)$$

Since, according to our homology modeling estimations, R ranges from 4.1 to 4.2 Å for OtCPF1 and OtCPF2, the upper limit of k (when $\Delta G = -\lambda$) should be of the order of 3×10^{-12} s^{-1}. This value is in good agreement with the experimental lifetimes (390 and 590 fs), which in turn indicates that $\Delta G = -\lambda$ approximately applies for the photoreduction of FAD_{ox} in OtCPF1 and OtCPF2. It can therefore be inferred that these primary reactions are nearly barrierless. A small barrier might explain the slightly slower reaction rate in EcCPD, for which R is equal to 4.3 Å.[55]

The lifetime corresponding to the second kinetic step (reduction of the proximal tryptophanyl radical by the medium tryptophan is 9 ps for OtCPF1 and, tentatively, 13 ps for OtCPF2) is in good agreement with lifetimes (ranging from 20 to 54 ps) reported by Kao et al. for the same reaction in other cryptochromes and photolyases.[25] These numbers could also agree well with the corresponding value (faster than 9 ps) deduced by the Brettel and Vos groups for EcCPD initially bearing $FADH^\bullet$.[23,24] It should be kept in mind, however, that the Brettel and Vos value of 9 ps is an upper limit and that the actual lifetime could be significantly smaller.

As far as the subsequent kinetic step is concerned (reduction of the medium tryptophanyl radical by the distal tryptophan in 81 ps in OtCPF1 and, tentatively, in 340 ps in OtCPF2), our values are significantly larger than the upper limit of 30 ps deduced by the Brettel and Vos groups for EcCPD initially bearing $FADH^\bullet$.[22] No precise value was given by Kao et al. although they mention a lifetime in the proximate nanosecond regime.[25]

In the absence of reliable crystallographic structures of our proteins (and those reported by Kao et al.[25]), it is difficult to rationalize the differences in the various reported lifetimes. We can generically invoke the fact that the distances between tryptophan residues, their relative orientations and the chemical nature of the amino-acid surrounding them (which may modulate their oxidation potential) can substantially alter the driving force of the electron hopping reaction. We in particular noticed that the loop surrounding the distal tryptophan (WH_d) residue in EcCPD (from H_{288} to P_{310}) is very different from that found in OtCPF1 or OtCPF2. In OtCPF1 and OtCPF2 this loop contains twice as many charged aminoacids than in EcCPD. The OtCPF2 loop contains more positively charged aminoacids than OtCPF1 and EcCPD. More precisely, in EcCPD WH_d closely interacts with one hydrophobic residue (V_{304}) and several carbonyl groups of the peptide backbone. According to our homology calculations, the nearest neighbors of WH_d in OtCPF1 are two hydrophobic residues (M_{462} and L_{471}) and the positively charged K_{475}. In our model of OtCPF2, WH_d mostly interacts with one hydrophobic residue (L_{341}) and two positively charged residues (R_{347} and R_{353}). The surrounding of the other tryptophans does not show such drastic differences between proteins. However, it is interesting to note that the proximal tryptophan (WH_p) of OtCPF2 is in π interaction with another tryptophan (W_{424}), whereas in OtCPF1 and EcCPD WH_p interacts with an asparagine. It might therefore be thought that such differences could explain the kinetic differences observed between the various chromoproteins.

5. Concluding Remarks

We have shown by femtosecond transient absorption spectroscopy that the ultrafast photoreduction of FAD_{ox} bound to two new CPF proteins (OtCPF1 and OtCPF2) from the green alga *O. tauri* occurs in the subpicosecond regime (390 fs for OtCPF1 and 590 fs for OtCPF2). For the first time in the case of oxidized CPF proteins the photoproducts of this reaction were spectroscopically identified, by full broadband transient spectra, as $FAD^{\bullet-}$ and $WH^{\bullet+}$. As this primary photoreaction is ultrafast, subsequent kinetic steps occurring in the picosecond regime could be resolved and interpreted. They are assigned to a cascade of electron hopping reactions along a chain of three conserved tryptophan residues, as reported by the groups of Brettel and Vos for the photoreduction of $FADH^\bullet$ within EcCPD.[18–24] Charge recombination reactions in competition with the electron hopping mechanism were identified as well.

Protein alignments allowed us to verify that the chain of tryptophan residues found in other CPF proteins is well conserved within OtCPF1 and OtCPF2. The spatial disposition of the tryptophan residues and the flavin found by homology modeling is very similar to the one experimentally reported for EcCPD.

In the case of OtCPF1 we could propose a complete kinetic model of the photoreduction reaction, including rate constants and electron transfer yields. The case of OtCPF2 is more complex, due a particular kinetic behavior that we attributed to the presence of a ground-state heterogeneity in the samples. One so-called reactive (FAD_{ox}) population undergoes the photoreduction mechanism through the tryptophan chain, while the nonreactive simply decays in 13 ps to the ground state. This population might correspond to FAD_{ox} being bound to OtCPF2 in the binding site of MTHF. A kinetic model, analogous to the one of OtCPF1, was tentatively proposed, but no rate constants were given due to the complexity of the system.

Polarized transient absorption experiments performed on OtCPF2 further allowed us to provide elements in favor of the electron hopping mechanism along the tryptophan chain and tentatively confirmed the fact that the final photoproduct observed in our experimental time window involves the radical cation of the distal tryptophan residue.

Supporting Information Available: (1) Spectroscopic chemical analysis of MTHF and FAD in OtCPF2; (2) total concentration of FAD and concentration of MTHF in OtCPF2; (3) global analysis of the transient absorption data of OtCPF1; (4) global analysis of the transient absorption data of OtCPF2; (5) reconstructed isotropic transient spectra of OtCPF2; (6) SVD analysis of the polarized transient spectra of OtCPF2; (7) photoreduction products of OtCPF1; (8) homology modeling; (9) ground-state heterogeneity of OtCPF2; (10) photoreduction products of OtCPF2. This material is available free of charge via the Internet at http://pubs.acs.org.

JA1002372